Reprinted from

Canadian Journal of Fisheries and Aquatic Sciences

Réimpression du

Journal canadien des sciences halieutiques et aquatiques



# Modeling tidal stress, circulation, and mixing in the Bristol Channel as a prerequisite for ecosystem studies

R. J. UNCLES

Volume 40 • Supplement Number 1 • 1983

8–19

Canada

Government of Canada
Fisheries and Oceans

Gouvernement du Canada
Pêches et Océans

Printed in Canada by K.G. Campbell Corporation

# Modeling Tidal Stress, Circulation, and Mixing in the Bristol Channel as a Prerequisite for Ecosystem Studies[1]

R. J. UNCLES

*Natural Environment Research Council, Institute for Marine Environmental Research, Prospect Place, The Hoe, Plymouth PL1 3DH, England*

UNCLES, R. J. 1983. Modeling tidal stress, circulation, and mixing in the Bristol Channel as a prerequisite for ecosystem studies. Can. J. Fish. Aquat. Sci. 40(Suppl. 1): 8–19.

A depth-averaged hydrodynamical numerical model is used to evaluate tidal stresses, currents, and mixing in the Bristol Channel and Severn Estuary. Benthic macrofaunal associations and sediment bed types are shown to depend on the magnitude of the tidal stress, and the direction of sediment transport (as bed-load) in the central parts of the Channel is shown to be a consequence of ebb dominated stress. This asymmetry in the tidal stress is mainly caused by $M_4$ currents, and computed $M_4$ elevations and currents are compared with observed values at a number of stations. Residual flows and horizontal mixing are deduced from the hydrodynamical model, and used to construct transport relationships for an ecosystem model. Agreement between observed salinity over a number of years and that computed by the ecosystem model is generally good.

*Key words*: Bristol Channel, hydrodynamical model, salinity model, tidal stress, $M_4$ tides, sediment movement

UNCLES, R. J. 1983. Modeling tidal stress, circulation, and mixing in the Bristol Channel as a prerequisite for ecosystem studies. Can. J. Fish. Aquat. Sci. 40(Suppl. 1): 8–19.

Un modèle numérique hydrodynamique à profondeur moyenne a servi à évaluer la pression des marées, les courants et le mélange dans le chenal de Bristol et l'estuaire de la Severn. On constate que les associations macrofauniques benthiques et les types de lits de sédiment dépendent de la pression des marées. On démontre aussi que la direction du transport des sédiments (comme charge de lit) dans les parties centrales du chenal résulte de la pression exercée surtout par le jusant. Cette asymétrie de pression exercée par la marée est causée en grande partie par des courants $M_4$, et nous comparons les élévations et courants $M_4$ avec les valeurs observées à un certain nombre de stations. Les flux résiduaires et le mélange horizontal sont déduits du modèle hydrodynamique et sont utilisés dans l'élaboration de relations de transport en vue d'un modèle d'écosystème. Il y a généralement bon accord entre la salinité observée pendant plusieurs années et celle calculée à l'aide du modèle d'écosystème.

Received October 14, 1981
Accepted August 31, 1982

Reçu le 14 octobre 1981
Accepté le 31 août 1982

TIDAL streams have a profound influence on the ecology of the Bristol Channel and Severn Estuary. Because of this, hydrodynamical numerical models of tidal flow have an important role to play in quantifying ecological processes in the region. The purpose of this paper is to use currents computed from such a model, in conjunction with field observations, to investigate the frictional drag on the seabed due to current flow (tidal stress), together with long-term, large-scale circulation of sediment (as bed-load), and water in the area. The relevance of these physical processes to estuarine ecology is emphasized. The philosophy behind this work is that fundamental studies of physical processes can profitably run in parallel with, and make important contributions to, research into estuarine and coastal marine ecology. Although current meter observations alone could provide the necessary background to some ecological studies, for many it is impossible to achieve the requisite geographical and temporal coverage of observational data. Under these circumstances the application of hydrodynamical models is essential.

Using a hydrodynamical model, it is shown that tidal stresses at the seabed not only govern sediment bed types and distributions of benthic macrofaunal associations (Warwick and Uncles 1980), but are also able to explain sediment transport paths for bed-load in the central part of the Bristol Channel (Belderson and Stride 1966). The work of Pingree and

[1]This paper forms part of the Proceedings of the Dynamics of Turbid Coastal Environments Symposium convened at the Bedford Institute of Oceanography, Dartmouth, N.S., Canada, September 29–October 1, 1981.

Printed in Canada (J6673)
Imprimé au Canada (J6673)

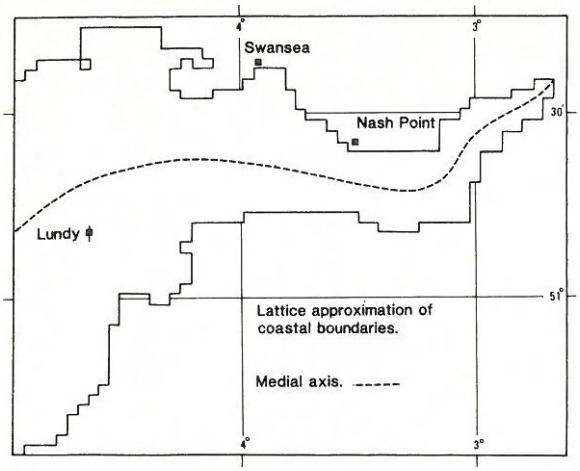


FIG. 1. Lattice approximation of coastal boundaries in the Bristol Channel and Severn Estuary (west and east, respectively, of Nash Point). The medial axis of the Channel (– – –).

Griffiths (1979) is extended to incorporate residual (tidally averaged) currents in the frictional drag law, as well as employing a much higher spatial resolution in the numerical model.

Applications of physical data to holistic ecosystem simulations entail a coarser description of the physical processes (both in time and space) than is obtained using hydrodynamical models. Here, the role of physical models is to advect and disperse biological and chemical components of the ecosystem through the region of interest and over the course of, perhaps, several years (Kremer and Nixon 1978). The long-term advection and dispersion of dissolved materials is influenced by tidally induced residual flows (Uncles 1982), which can be derived from hydrodynamical models. However, an empirical approach must generally be used to quantify the transport for ecosystem studies. Such an approach is outlined for the Bristol Channel and, as illustration of its capabilities, is used to compute distributions of salinity over the region. Comparisons of computed with observed distributions of salinity over a number of years are presented.

The hydrodynamical model uses finite-difference methods to solve the well-known depth-averaged equations of continuity and momentum in their standard nonlinear forms (Tee 1976; Pingree and Maddock 1977). The effect of buoyancy due to horizontal density gradients is taken into account; the coefficient of horizontal eddy viscosity is taken to be $10^6$ cm$^2 \cdot$s$^{-1}$ (Tee 1976), and the drag coefficient, $k$, in the quadratic friction law is $2.5 \times 10^{-3}$. A (53 × 43) lattice of points is used with a uniform spacing of 3.1 km (see Fig. 1). The Bristol Channel and Severn Estuary are arbitrarily defined here as the regions west and east of Nash Point in Fig. 1. Although not shown in Fig. 1, the upper reaches of the model Severn are extended further towards the head by 15 km, using a one-dimensional approximation of the estuary. The conditions on water level specified at the seaward boundary are the residual (tidally averaged) surface elevation relative to Ordnance Datum (Newlyn), and the amplitudes and phases of the $M_2$ and $M_4$ tides (the principal lunar semidiurnal and quarter-diurnal tidal heights). The $M_2$ elevations and currents derived from the model are in good agreement with observations (Uncles 1981a).

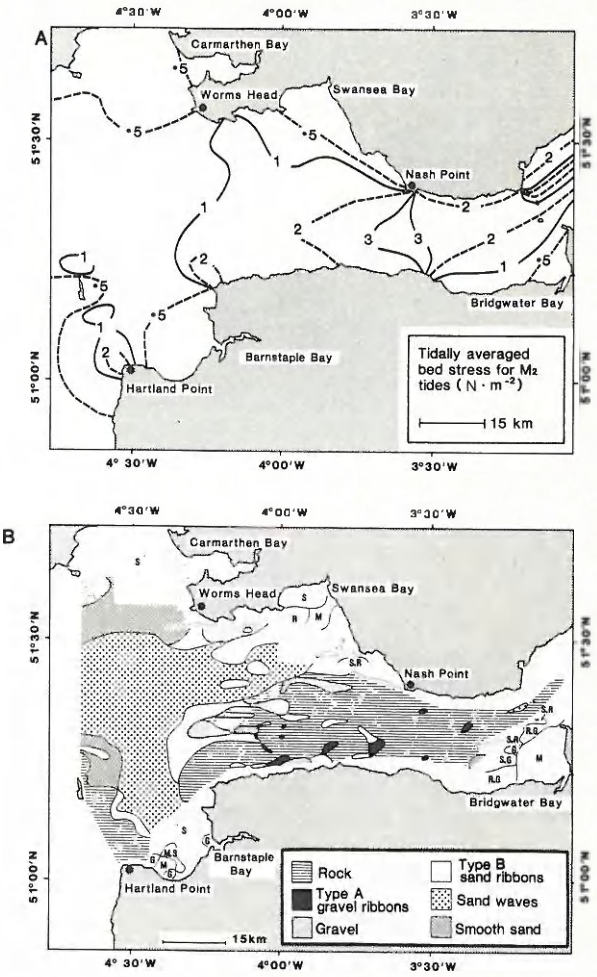


FIG. 2. Tidally averaged magnitude of seabed stress for $M_2$ tides, and sediment bed types: A, stress (N·m$^{-2}$); B, Bed types, R(rock), G(gravel), S(sand), M(mud). Linear sand banks are drawn in.

## Tidal Stress

Using the quadratic formulation, the tidal stress on the seabed due to frictional drag of water flowing over it may be written:

$$\boldsymbol{\tau} = \rho k \mathbf{v}|\mathbf{v}|, \quad (1)$$

where $\rho$ is the density of seawater, $k$ is the drag coefficient and $\mathbf{v}$ is the depth-averaged current; its magnitude is:

$$|\boldsymbol{\tau}| = \rho k |\mathbf{v}|^2. \quad (2)$$

Both equations can be easily evaluated from the hydrodynamical model of the Channel. Averaging equation (2) over a tidal cycle yields the tidally averaged magnitude of the stress, $\langle|\boldsymbol{\tau}|\rangle$, which is contoured in Fig. 2A for the case of $M_2$

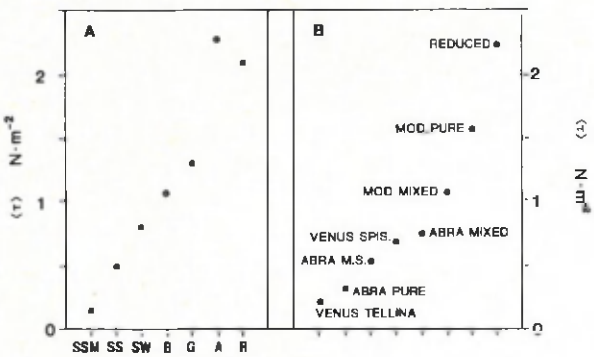


FIG. 3. Bed types and benthic macrofaunal associations against tidally averaged magnitude of bed stress for $M_2$ tides: A, Bed types, R(rock), A(type A gravel ribbons), G(smooth gravel), B(type B sand ribbons), SW(sand waves), SS(smooth sand), SSM(smooth sand and mud); B, Benthic macrofaunal associations.

tidal streams. Peak tidal stresses occur during maximum flood and ebb tidal streams, and these are approximately twice the values shown in Fig. 2A owing to the fact that the tidal currents at each point are essentially rectilinear, and approximately sinusoidal with time (Uncles 1981a).

The effect of tidal stress on the substrate is evident from Fig. 2B, which shows the distribution of sediment bed types in the Bristol Channel and western Severn Estuary. The region of high stress in the eastern Bristol Channel is a zone of erosion with a rock bed; gravel accumulates in the lower stress region seaward of the zone, and may form gravel ribbons (Type A of Kenyon 1970). The western part of the Channel is a region of large sand waves, which adjoins areas of smooth sand to the south and north, and which is separated from the gravel and rock areas to the east by thin sand ribbons (Type B of Kenyon 1970). In Bridgwater Bay (Fig. 2B), and further up the estuary, sediment bed types are governed by the dense suspensions of particulate material maintained in the water column by the strong currents.

Data from Fig. 2(A, B) have been synthesized in Fig. 3A, which shows each bed type as a function of the mean residual (tidally averaged) tidal stress for which it occurs. There is a fairly smooth progression from high tidal stresses associated with the rock bed and gravel ribbons, through the intermediate stress values producing movement of sand waves, to the low stresses resulting in permanent deposition of sediment to form beds of smooth sand and muddy sand. A similar correlation is illustrated in Fig. 3B for tidal stress and benthic faunal types in the Bristol Channel, and this correlation has been considered in detail by Warwick and Uncles (1980).

According to Belderson and Stride (1966), the direction of sand transport in the Channel (as bed-load) is from the zone of erosion to the Celtic Sea. Generally, the instantaneous rate of sand transport varies as the current speed raised to some power, which is typically about four. This means that most of the transport occurs near peak flood or ebb currents (ignoring wind–wave effects). Any significant difference in the magnitudes of the peak flood and ebb currents (the asymmetry) will therefore largely determine the residual transport of sand. Tidal asymmetry in the currents has been investigated in detail for the Severn Estuary (Uncles 1981b). If infinitely repeating

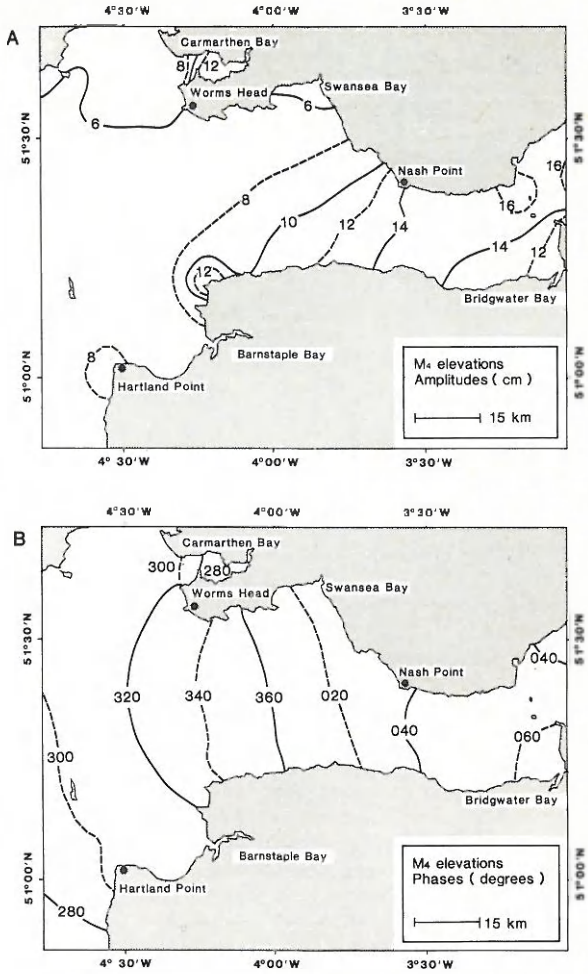


FIG. 4. $M_4$ elevations: A, Amplitudes (cm); B, Phases (degrees).

$M_2$ tides are considered as being representative of average tidal conditions in the Channel, then tidal asymmetry is produced mainly by residual (tidally averaged) currents, and by $M_4$ tides. The effects of higher overtides ($M_6$, $M_8$, ...) are irrelevant or small. Therefore, the hydrodynamical model has been used to investigate $M_4$ tides in the Channel from a fundamental viewpoint, as well as to identify possible transport paths for sediment bed-load directly from the computed tidal currents.

## $M_4$ TIDES

Seaward boundary conditions for the $M_4$ elevations were derived from a coarse grid model of the southwest shelf (Miles 1979). The amplitudes and phases of the $M_4$ tide, according to the hydrodynamical model, are contoured in Fig. 4A and B, respectively. These values were derived by running the model over a number of tidal cycles until periodic solutions were obtained. Fourier analysis of the computed water elevations and velocities then gave the $M_2$, $M_4$, and residual properties. For velocity:

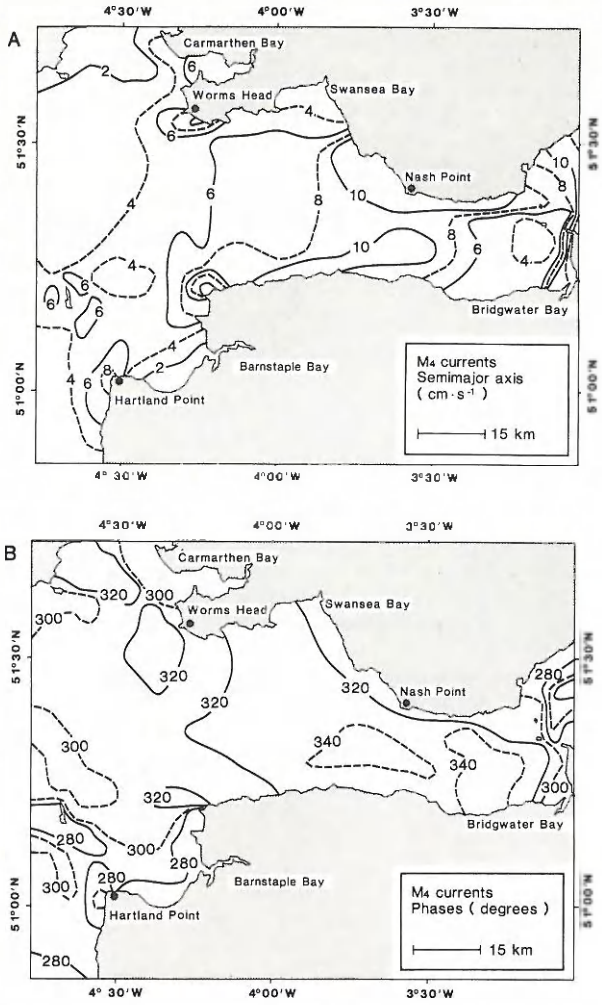


FIG. 5. $M_4$ currents: A, Maximum currents (semimajor axis), $cm \cdot s^{-1}$; B, Phases (degrees).

$$\mathbf{v} = \langle \mathbf{v} \rangle + \mathbf{v}_2 + \mathbf{v}_4 + \ldots$$

where $\mathbf{v}_2$ is the $M_2$ current, and $\langle \mathbf{v} \rangle$ and $\mathbf{v}_4$ are the much smaller residual and $M_4$ currents. The amplitudes of the $M_4$ elevations increase from about 6 cm in the west to 14 cm in the mouth of the Severn (located at Nash Point, Fig. 4A). The increase in elevation continues towards the head of the Severn. Enhanced elevations occur near headlands due to centrifugal effects (see also Pingree and Maddock 1978). The computed $M_4$ tide is the sum of contributions due to local nonlinear generation (Pingree and Maddock 1978; Uncles 1981b), and the presence of an $M_4$ wave propagating into the Channel from the Celtic Sea, where it is amplified by funnelling. The phases of the $M_4$ elevations in Fig. 4B are proportional to the time of maximum elevation for the $M_4$ tide. These show propagation into the Channel until Bridgwater Bay; thereafter the propagation is down-estuary, indicating large local generation in the upper reaches of the Severn.

The head of the depth averaged $M_4$ current vector describes an ellipse during the course of an $M_4$ tidal period of 6.2 h. The

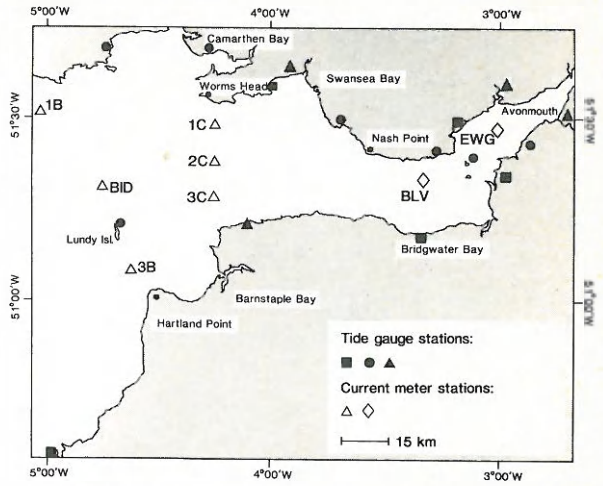


FIG. 6. Tide-gauge stations at which measurements have been made for 15 d, 1 mo, and 1 yr are shown as ■, ●, and ▲, respectively. Stations at which two or three recording current meters were deployed on a mooring for 1 mo are shown (△). Near-surface current measurements extending over 1 mo are shown (◇). Data at station BID courtesy of M. J. Howarth (personal communication).

maximum currents have magnitude $a_4$, and define the semimajor axis of the ellipse. The orientation of the ellipse, $\delta_4$, is the direction of the maximum current ($a_4$) in an up-channel sense. The maximum up-channel current is reached at a time $t = e_4/\omega_4$, where $e_4$ is the phase of the current, and $\omega_4$ the angular frequency of the $M_4$ tide ($57.97°h^{-1}$). The $M_4$ currents reach minimum values one quarter of a period after they reach maximum values. The minimum currents have magnitude $b_4$, and define the semiminor axis of the ellipse. The semiminor axis is positive if the head of the current vector is moving cyclonically around the ellipse, and is negative if it is moving anticyclonically.

The maximum $M_4$ currents ($a_4$, the semimajor axes of the $M_4$ tidal current ellipses) are shown in Fig. 5A. Large values occur near headlands, which is again due to centrifugal effects, and currents increase progressing up-channel due to funnelling and local nonlinear generation. The region of low currents near Bridgwater Bay results from opposing phases of the up-estuary travelling, and locally generated $M_4$ tides. Phases of the $M_4$ currents ($e_4$) are contoured in Fig. 5B, which has been drawn to show less detail in the bays than is evident from the model. Propagation is again shown to be up-channel seawards of Bridgwater Bay, and down-channel further into the Severn.

## COMPARISON WITH OBSERVATIONS

Some of the results for $M_4$ tides can be compared with observations. Positions at which tidal heights and currents have been measured are drawn in Fig. 6.

The comparisons between observed and computed $M_4$ elevation amplitudes and phases are given, respectively, in Fig. 7A and 7B. The agreement is reasonable at the lower amplitudes (<15 cm, relative accuracy 16%) and phases (<20°, relative accuracy 13%) of the Bristol Channel, but

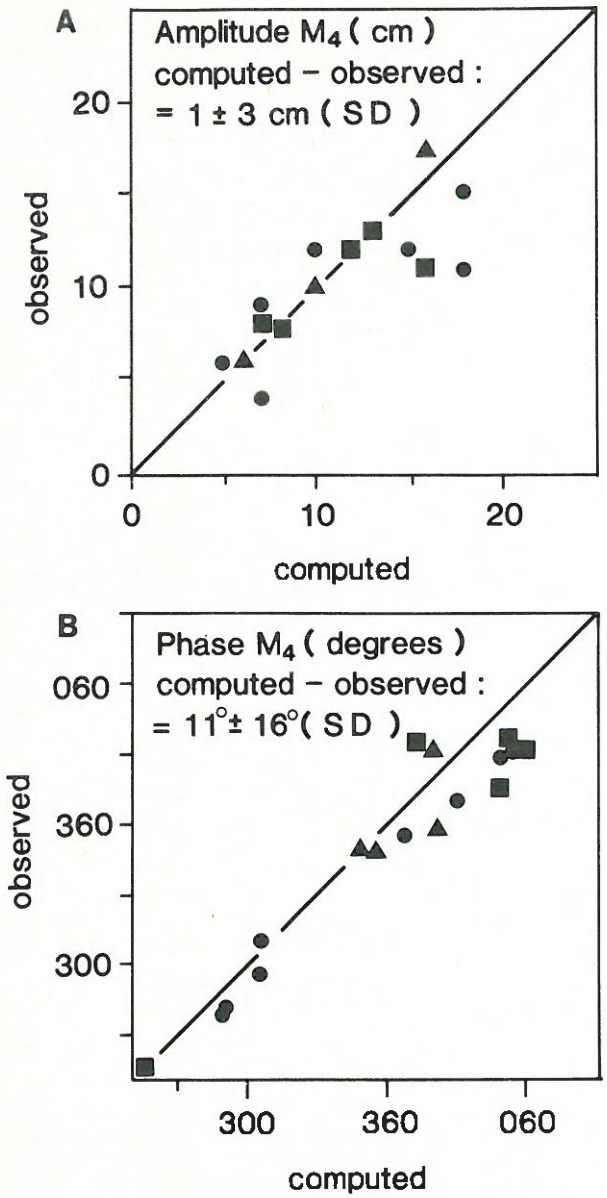


FIG. 7. Observed against computed $M_4$ elevations: A, Amplitudes (cm); B, Phases (degrees).

both the computed amplitudes and phases are too large in the Severn. Although not shown in Fig. 7A, the computed amplitude at Avonmouth (see Fig. 6 for location) is 45 cm, while the observed value is only 34 cm. Thus, the two-dimensional simulation of $M_4$ tides becomes inaccurate in the upper Severn, presumably because of its poor resolution of topography (especially depth) in the upper reaches, where local generation of $M_4$ tides is important. Prandle (1980) found similar excessive generation of $M_4$ tide at the head of both the Severn and Thames, and attributed this to inaccuracies in the computed frictional effects in shallow water.

Observed and computed properties of the $M_4$ tidal currents are compared in Table 1. One-month stations are used (△ and ◇ in Fig. 6), and tidal ellipse data for all current meters on a mooring are averaged. With the exception of station 2C in Table 1, the computed semimajor and semiminor axes (the maximum and minimum $M_4$ currents, $a_4$ and $b_4$) are within 1 cm·s$^{-1}$ of the observed values. Computed and observed phases of the $M_4$ currents, $e_4$, are generally in agreement to within 10°–20° (~10–20 min), and a similar agreement exists for the orientations of the tidal ellipses, $\delta_4$.

TABLE 1. Observed and computed, (•), properties of $M_4$ tidal ellipses. Semimajor axis, $a_4$, semiminor axis, $b_4$, phase relative to Greenwich, $e_4$, orientation relative to north, $\delta_4$. $\phi = 2e_2 - e_4$.

| Station | $a_4$ cm·s$^{-1}$ | $b_4$ cm·s$^{-1}$ | $e_4$ degrees | $\delta_4$ degrees | cos ($\phi$) |
|---|---|---|---|---|---|
| 1B | 3(3) | −1(0) | 273(276) | 40(60) | −0.7(−0.6) |
| 3B | 3(4) | 1(1) | 303(297) | 41(42) | −0.1(−0.4) |
| 1C | 5(6) | 1(0) | 323(317) | 84(102) | −0.8(−0.7) |
| 2C | 3(6) | 0(−1) | 334(321) | 60(81) | −1.0(−0.7) |
| 3C | 5(6) | −1(−2) | 328(313) | 71(80) | −0.8(−0.6) |
| BID | 2(3) | 0(−1) | 289(297) | 53(66) | −0.5(−0.7) |
| BLV | 5(5) | — | 367(341) | 92(92) | −0.9(−0.6) |
| EWG | 11(12) | — | 262(250) | 57(56) | 0.9(1.0) |

The maximum $M_2$ and $M_4$ tidal currents tend to be aligned in the same direction with their respective tidal ellipse semimajor axes pointing along the medial axis of the Channel (see Fig. 1). Assuming that the maximum $M_4$ and $M_2$ currents are parallel, and that the cross-channel currents (the tidal ellipse semiminor axes) are negligible, then the $M_4$ currents reinforce either the flood or ebb streams according to whether cos$\phi$ is greater or less than zero, where:

$$\phi = 2e_2 - e_4, \tag{3}$$

and where $e_2$ is the phase of the $M_2$ currents. The peak $M_4$ flood current, $a_4$, leads the peak $M_2$ flood current, $a_2$, by a time $\phi/\omega_4$, where $\omega_4$ is twice the angular frequency of the $M_2$ tide.

In Table 1, cos$\phi$ is compared for computed and observed currents. The agreement is reasonable, and shows that the summation of $M_2$ and $M_4$ currents produces ebb dominated flows (cos$\phi$ < 0) at all stations except EWG (see Fig. 6), which is some considerable distance into the Severn (see also Uncles 1981b).

## RESIDUAL AND MAXIMUM TIDAL STRESSES

As a first approximation the Bristol Channel can be treated as a one-dimensional system, with currents and spatial gradients occurring only along its medial axis (see Fig. 1), so that $b_2 = 0 = b_4$. In this case the residual tidal stress on the seabed due to the sum of $M_2$ and $M_4$ currents is approximately (see equation (1) and Uncles 1981b):

$$\langle\tau\rangle' = \rho k\langle(\mathbf{v}_2 + \mathbf{v}_4)|\mathbf{v}_2 + \mathbf{v}_4|\rangle \simeq \frac{4}{3\pi}\hat{\mathbf{x}}\rho k a_2 a_4 \cos\phi. \tag{4}$$

Here, $\hat{\mathbf{x}}$ is a unit vector directed up-channel along the medial axis in Fig. 1, and $\phi$ is given by equation (3). In one dimension, the residual tidal stress due to the sum of $M_2$ and residual currents is approximately (Uncles 1981b):

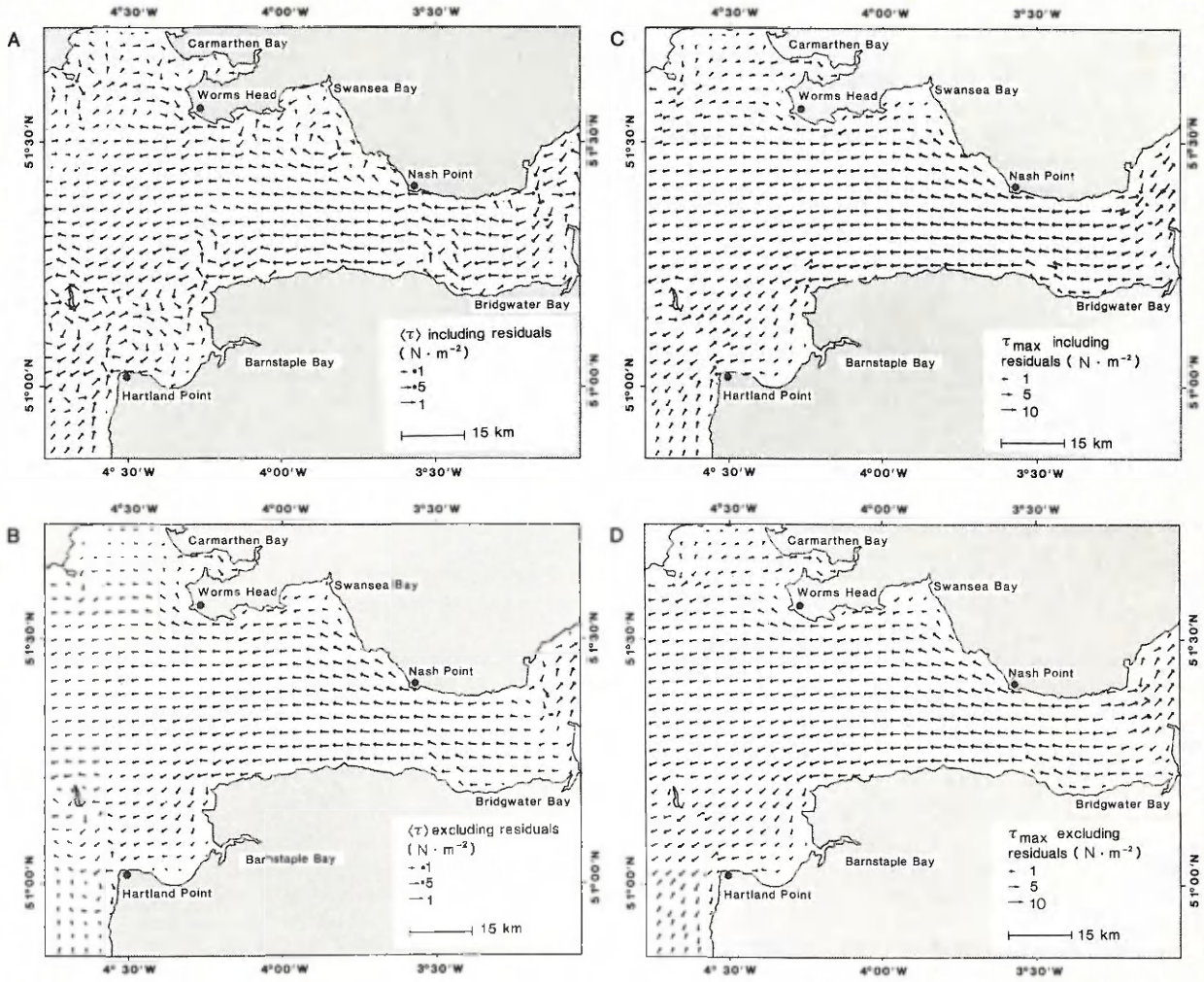


FIG. 8. Residual and maximum seabed tidal stresses $\langle\boldsymbol{\tau}\rangle$ and $\boldsymbol{\tau}_{max}$ ($N \cdot m^{-2}$): A, Residual stress, $\langle\boldsymbol{\tau}\rangle$, including residual currents; B, Residual stress, $\langle\boldsymbol{\tau}\rangle$, excluding residual currents; C, Maximum tidal stress, $\boldsymbol{\tau}_{max}$, including residual currents; D, Maximum tidal stress, $\boldsymbol{\tau}_{max}$, excluding residual currents.

$$(5) \qquad \langle\boldsymbol{\tau}\rangle'' = \rho k\langle(\mathbf{v}_2 + \langle\mathbf{v}\rangle)|\mathbf{v}_2 + \langle\mathbf{v}\rangle|\rangle \simeq \frac{4}{\pi}\rho k a_2\langle\mathbf{v}\rangle.$$

From equations (1), (4) and (5) the total residual tidal stress is:

$$\langle\boldsymbol{\tau}\rangle = \rho k\langle\mathbf{v}|\mathbf{v}|\rangle \simeq \langle\boldsymbol{\tau}\rangle' + \langle\boldsymbol{\tau}\rangle''.$$

In two dimensions, the total residual tidal stress due to overtides and residual currents, $\langle\boldsymbol{\tau}\rangle$, can be computed directly from the hydrodynamical model using equation (1). The distribution of $\langle\boldsymbol{\tau}\rangle$ is shown in Fig. 8A. Outside of the bays, in the deeper, central parts of the Channel, the residual tidal stress is directed from east to west. If the residual transport of sand as bed-load were determined by the residual tidal stress, then the expected sediment transport paths would be from the zone of erosion (shown in Fig. 2B), across the sand wave field to the Celtic Sea. This is in agreement with the results of Belderson and Stride (1966).

Residual currents which have been computed here using a depth averaged model may be different from those which flow near the seabed in nature (Uncles 1982), and which are able to affect sediment movement. Therefore, it is important to investigate the sensitivity of the computed distribution of residual tidal stress to the residual current flow. If the computed residual currents, $\langle\mathbf{v}\rangle$, are subtracted from the computed total currents, $\mathbf{v}$, before the stress is evaluated in equation (1), then the residual tidal stress is solely the result of $M_2$, $M_4$, and higher overtide interactions, and is given approximately by $\langle\boldsymbol{\tau}\rangle'$ in equation (4). Actual values of $\langle\boldsymbol{\tau}\rangle'$ from the model are drawn in Fig. 8B. Except in the bays and in the upper Severn, the exclusion of residual current flow has no qualitative effect on the residual tidal stress.

Maximum tidal stress, $\boldsymbol{\tau}_{max}$, occurs at the time of maximum water velocity, $|\mathbf{v}|_{max}$, and is given by equation (1) with $|\mathbf{v}| = |\mathbf{v}|_{max}$. The magnitude and direction of maximum stresses computed from the model are shown in Fig. 8C. The maximum stress depends primarily on the summation of the $M_2$, $M_4$, and residual currents. If the residual transport of sand

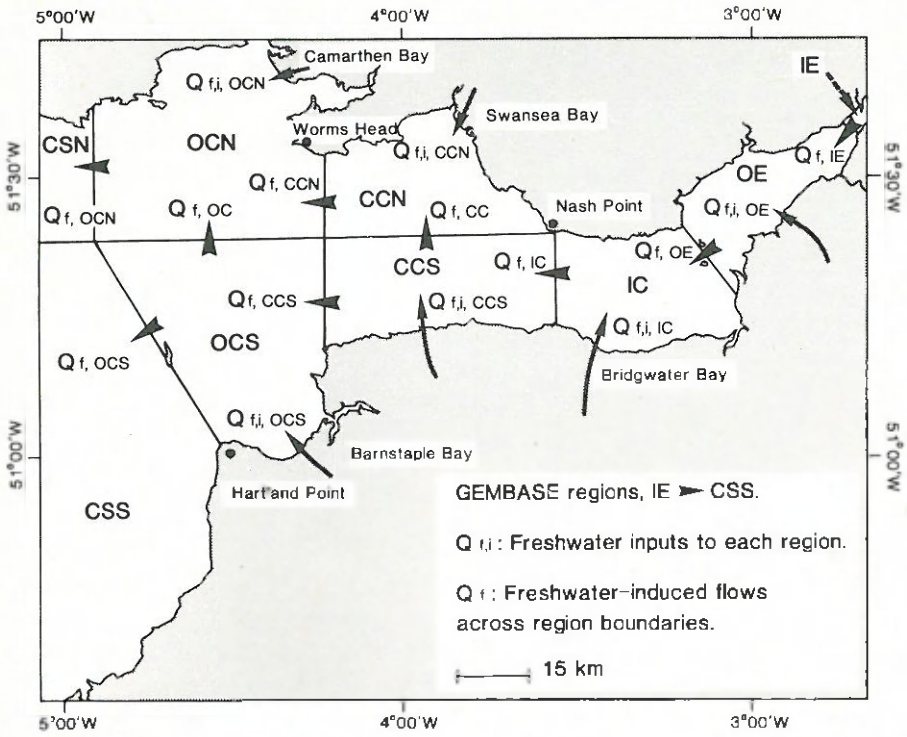


FIG. 9. Regions used in the GEMBASE model, showing freshwater inputs to each region, $Q_{f,i}$, and freshwater-induced flows across region boundaries, $Q_f$. Inner Estuary (*IE*); Outer Estuary (*OE*); Inner Channel (*IC*); Central Channel South and North (*CCS* and *CCN*); Outer Channel South and North (*OCS* and *OCN*); Celtic Sea South and North (*CSS* and *CSN*).

as bed-load were determined by the maximum tidal stress, then the expected sediment transport paths in the central parts of the Channel would again be from the zone of erosion (Fig. 2B), across the sand wave field to the Celtic Sea.

Figure 8D shows the maximum tidal stresses, $\tau_{max}$, calculated in the model when computed residual currents are subtracted from the computed total currents before $\tau_{max}$ is evaluated from equation (1). In this case, maximum stresses depend primarily on the summation of $M_2$ and $M_4$ currents. The results of calculating $\tau_{max}$ including and excluding residual currents in equation (1) (Fig. 8C and 8D) are qualitatively the same in the region of bed-load sediment transport.

Similar results on the direction of sediment transport as bed-load can be inferred from work by Pingree and Griffiths (1979), who computed tidally averaged and peak stresses due solely to $M_2$ and $M_4$ interactions, using a coarse lattice model of the U.K. shelf. The present work has extended this to include the effects of residual flows, and to compute the stresses over a much finer lattice for the Bristol Channel. The problems of suspended sediment transport, both tidal and wind–wave induced, and sediment supply, have not been addressed.

## Transport Equations for Ecological Modeling

The numerical model GEMBASE (general ecosystem model of the Bristol Channel and Severn Estuary) computes the interactions between biological and chemical variables during mixing and advection by tidal and residual currents (Radford 1979, 1981; Radford and Joint 1980; Joint 1983). The nine regions used in the GEMBASE model are named and depicted schematically in Fig. 9. Freshwater inputs to each GEMBASE region, denoted by $Q_{f,i}$, are also shown in Fig. 9; on average, the river inputs from the Severn Estuary contribute about 60% of the total flow of freshwater to the Bristol Channel, while inputs from the northern and southern coastlines of the Bristol Channel amount to about 30 and 10%, respectively. Additional inputs of freshwater, due to the excess of precipitation over evaporation, are small compared with river inputs, and have been neglected.

Boundary conditions for GEMBASE are applied at the Inner Estuary (*IE*), and at the Celtic Sea North (*CSN*) and Celtic Sea South (*CSS*) regions (see Fig. 9). The boundary between the Celtic Sea North (*CSN*) and Outer Channel North (*OCN*) is 6 km up-channel from the seaward boundary of the hydrodynamical model (see Fig. 1). The remaining six modelled regions were chosen as a minimum set to describe the spatially differing ecological and physical properties of the Channel; a larger number of regions would have required excessive computer time to run the model through several years of simulated time for the many numerical experiments of interest.

The problem considered here is the determination of mixing

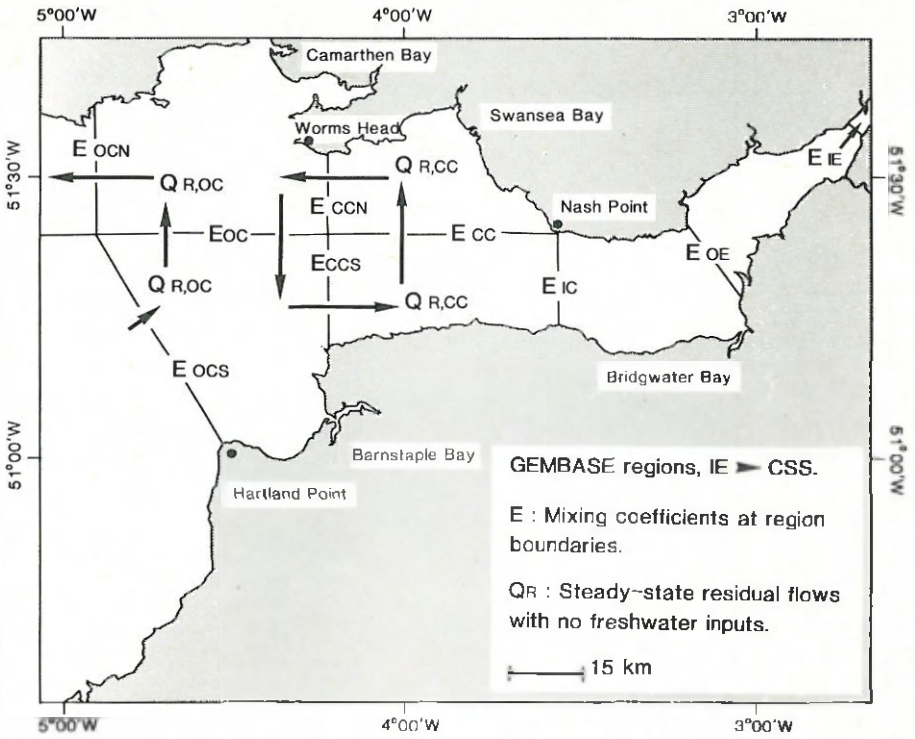


FIG. 10. Mixing coefficients at region boundaries, $E$, and steady-state residual flows with no freshwater inputs, $Q_R$.

and advection of water and dissolved materials between, and through, the large GEMBASE regions shown in Fig. 9, for periods of time of the order of several years. Both the spatial and temporal scales are much larger than those associated with the hydrodynamical numerical model of the Bristol Channel, so that some form of interfacing must be devised between the two types of models. The method devised for GEMBASE is not ideal because it relies, in part, on the calculation of residual flows and dispersion, neither of which are fully understood in estuaries subjected to strong tidal currents. However, the method has the advantages of being conceptually simple, rapid to run, and capable of generating realistic rates of transport between regions, as judged from the comparison of computed and observed distributions of freshwater in the Channel. Use is also made of the long-term salt balance, which, while being insufficient to define transport over the two-dimensional Bristol Channel regions shown in Fig. 9, is able to do so in the one-dimensional regions which represent the Severn Estuary (Uncles and Radford 1980; Radford et al. 1981).

## ADVECTION AND MIXING

The transport of salt and water across any boundary between two GEMBASE regions in Fig. 9 is considered. The instantaneous rate of transport of water, $Q$, across the boundary is:

$$(6) \quad Q = A\bar{u}$$

where the overbar denotes an average over the boundary's area, $A$, and where $u$ is the component of depth averaged velocity, $\mathbf{v}$, perpendicular to $A$.

The associated transport of salt is:

$$(7) \quad F = A\overline{\bar{u}\bar{s}} = A\bar{u}\bar{s} + A\overline{u's'}$$

Here, the prime denotes a deviation from the cross-sectional average; for example, $s = \bar{s} + s'$. The residual rate of transport across $A$ follows from equations (6) and (7):

$$(8) \quad \langle F \rangle = \langle Q \rangle \langle \bar{s} \rangle + \{\langle \tilde{Q}\tilde{s} \rangle + \langle A\overline{u's'} \rangle\},$$

where $Q = \langle Q \rangle + \tilde{Q}$ and $\bar{s} = \langle \bar{s} \rangle + \tilde{s}$ — the tildes denoting cross-sectionally averaged tidal fluctuations.

The residual transport of water can be separated into two parts: one ($Q_f$) is due to freshwater inputs to the Channel (for example, $Q_{f,CC}$ is shown as flowing from the Central Channel South ($CCS$) to the Central Channel North ($CCN$) in Fig. 9), and the other results from all other mechanisms, $Q_R$:

$$\langle Q \rangle = Q_f + Q_R,$$

so that the residual transport of salt across $A$ is:

$$(9) \quad \langle F \rangle = Q_f S + Q_R S + \{\langle \tilde{Q}\tilde{s} \rangle + \langle A\overline{u's'} \rangle\},$$

where $S = \langle \bar{s} \rangle$.

An empirical mixing coefficient, $E$, is defined by:

$$(10) \quad E = -\{\langle \tilde{Q}\tilde{s} \rangle + \langle A\overline{u's'} \rangle\} / \delta S,$$

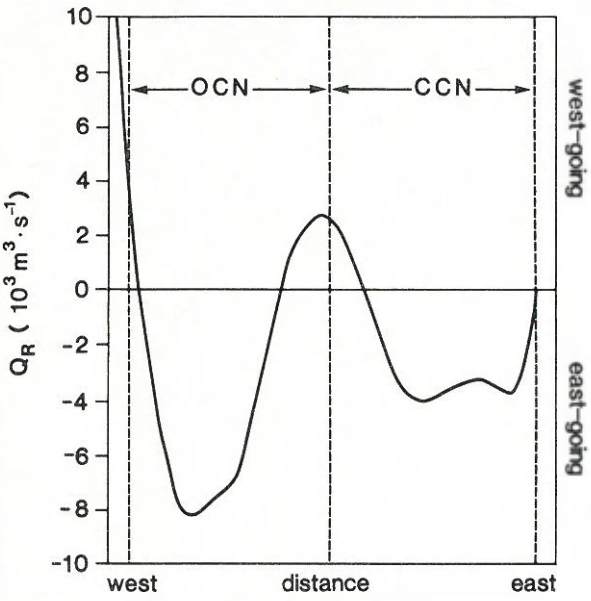


FIG. 11. Total west-going residual flow of water, $Q_R$, through the Outer Channel North and Central Channel North, according to the hydrodynamical model.

in which $\delta S$ is the difference in tidally averaged salinity between the two GEMBASE regions under consideration. Equation (9) becomes:

$$\langle F \rangle = Q_f S + Q_R S - E\delta S. \quad (11)$$

## RESIDUAL FLOWS

The freshwater flows across region boundaries in Fig. 9 can be determined from the hydrodynamical model. As the freshwater from each source enters a region it produces a head of water which drives currents out of the Channel. These currents are extremely small compared with the tidal flows, so that flow patterns can be investigated for each input of freshwater, and then summed to take into account all inputs according to:

$$\mathbf{Q}_f = \mathbf{B} \cdot \mathbf{Q}_{f,i}, \quad (12)$$

where $\mathbf{B}$ is a constant (9 × 9) matrix, $\mathbf{Q}_f$ are the flows $Q_{f,IE}$ to $Q_{f,OCS}$, and $\mathbf{Q}_{f,i}$ are the inputs $Q_{f,IE}$ to $Q_{f,OCS}$ (see Fig. 9).

Residual flows, $Q_R$, are shown in Fig. 10, together with mixing coefficients, $E$, which are defined at region boundaries. The residual flow from the Central Channel South to North is $Q_{R,CC}$, and that from the Outer Channel South to North is $(Q_{R,OC} - Q_{R,CC})$. $Q_R$ was computed from the hydrodynamical model, and is the residual flow due to $M_2$ tidal nonlinearities and density currents (Uncles 1982). Wind-driven currents have not yet been incorporated in GEMBASE, and the extent to which they contribute to the seasonal variability of the ecosystem is not known.

The residual flow of water through the Outer Channel North and the Central Channel North, according to the hydrodynamical model, is drawn in Fig. 11. The spatial variability of $Q_R$ is large, and $Q_{R,CC}$ and $Q_{R,OC}$ are, unfortunately, sensitive to the locations of the GEMBASE region boundaries. A schematic picture of the large-scale residual circulation, according to the hydrodynamical model, is drawn in Fig. 12.

## MASS BALANCE

The tidally averaged mass of salt in a GEMBASE region of volume $v$ is:

$$M_s = \langle v\bar{\bar{s}} \rangle$$

where $\bar{\bar{s}}$ is an average over $v$. If a tilde is now used to denote a volume averaged tidal fluctuation, then $M_s$ may be written:

$$M_s = \langle v \rangle \langle \bar{\bar{s}} \rangle \cdot [1 + \langle \tilde{v}\tilde{s} \rangle / \langle v \rangle \langle \bar{\bar{s}} \rangle] \simeq VS,$$

using $V = \langle v \rangle$, $S = \langle \bar{\bar{s}} \rangle$ and estimating $\langle \tilde{v}\tilde{s} \rangle / VS \sim 10^{-3}$.

The mass balance for salt in the Central Channel South, using equation (11) and with reference to Fig. 9 and 10 may therefore be written:

$$\begin{aligned} V_{CCS}\frac{d}{dt}(S_{CCS}) = &+ [Q_{f,IC}(S_{IC} + S_{CCS})/2 \\ &- E_{IC}(S_{CCS} - S_{IC})] \\ &- [(Q_{f,CCS} - Q_{R,CC})(S_{OCS} + S_{CCS})/2 \\ &- E_{CCS}(S_{OCS} - S_{CCS})] \\ &- [(Q_{f,CC} + Q_{R,CC})(S_{CCN} + S_{CCS})/2 \\ &- E_{CC}(S_{CCN} - S_{CCS})] \end{aligned} \quad (13)$$

A similar equation holds for each GEMBASE region, and for each variable subjected to advection and mixing — source terms being added to equation (13) to account for possible growth or decay.

## ESTIMATES FOR MIXING

$Q_f$ and $Q_R$ have been determined for use in equation (13); the mixing coefficients, $E$, are more difficult to compute. The method used to estimate $E$ is based on the satisfaction of equation (13). If equation (13) is averaged over a number of years, then $S$ will represent the long-term average salinity for each GEMBASE region, with $dS/dt = 0$, and $Q_R$ and $Q_f$ will represent the long-term flows. Thus, all of the extensive salinity data for each region in Fig. 9 were averaged to yield long-term values. For the Outer Estuary and Inner Channel the balance is given by equation (11) with $Q_R = 0$ and $\langle F \rangle = 0$ (see also Uncles and Radford 1980), so that:

$$E = Q_f S/\delta S \quad (14)$$

yielding $E_{IE}$, $E_{OE}$, and $E_{IC}$. In the two-dimensional region there are six mixing coefficients, $E_{CC}$ to $E_{OCS}$ (see Fig. 10), and only four equations of the form of equation (13) — one for each region. Therefore, two values of $E$ must be estimated directly from the hydrodynamical model, using equation (10) in conjunction with the long-term averaged salinity data. The flux in equation (10) consists of a part due to tidal pumping, $\langle \bar{Q}\bar{s} \rangle$, and a part due to transverse shear in the tidal and residual currents. Following Fischer et al. (1979), the effect of tidal shear can be shown to be negligible. The flux due to shear in the residual currents is:

$$\langle \overline{Au's'} \rangle = \langle A \rangle \langle \overline{u'}\overline{(s')} \rangle, \quad (15)$$

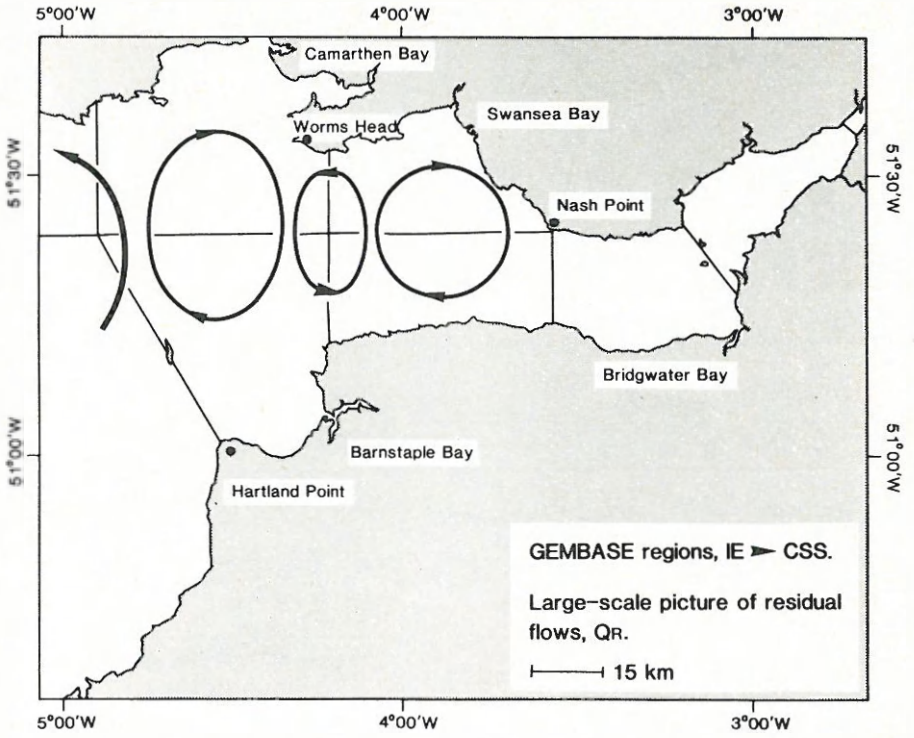


FIG. 12. Large-scale residual circulation, $Q_R$, in the Bristol Channel.

where, to take into account the Stokes drift (Uncles and Jordan 1979), $\langle u' \rangle$ must be computed as:

$$\langle u' \rangle = \{\langle Hu \rangle - \langle \overline{Hu} \rangle\} / \langle H \rangle,$$

and where the cross-sectional average is over $\langle A \rangle$, $H$ being the instantaneous depth. The effects of tidal pumping cannot be estimated with any certainty, and are ignored; therefore, equations (10) and (15) give:

$$(16) \quad E = -\langle A \rangle \langle \overline{u'} \langle s' \rangle \rangle / \delta S,$$

which can be computed using $\langle u' \rangle$ from the hydrodynamical model, and using $\langle s' \rangle$ and $\delta S$ from the long-term averaged salinity data.

In principle, $E$ could be derived from equation (16) for each boundary between GEMBASE regions. However, the current shear along those boundaries which terminate on headlands are dominated by the small intense circulation patterns near the headlands (for example, boundaries with mixing coefficients $E_{CCS}$ and $E_{OCS}$ in Fig. 10); because the observed salinity is determined on a lattice which has only one third the resolution of the hydrodynamical model (9 km as opposed to 3 km), the shear flux of salt in these headland circulations cannot be computed with accuracy. Also, the boundary between the Outer Channel North (*OCN*) and the Celtic Sea North (*CSN*) in Fig. 9 is very close to the seaward boundary of the hydrodynamical model, and may be subject to possible spurious boundary circulation patterns (Prandle 1978) and their associated shear. Finally, in view of the very small salinity difference ($\delta S = 0.22‰$) between the Central Channel North (*CCN*) and the Central Channel South (*CCS*), it was decided to compute $E_{CC}$ from the observed salt balance. Therefore, $E_{CCN}$ and $E_{OC}$ were computed directly from equation (16); the method yields a shear flux of salt into the Central Channel North (*CCN*) from the Outer Channel North (*OCN*) in Fig. 9 of 517‰ $m^3 \cdot s^{-1}$, which with $\delta S = 0.98‰$ gives:

$$E_{CCN} = 5 \times 10^2 \text{ m}^3 \cdot \text{s}^{-1}.$$

The computed shear flux from the Outer Channel South (*OCS*) to the Outer Channel North (*OCN*) in Fig. 9 is 2310‰ $m^3 \cdot s^{-1}$, which with $\delta S = 0.72‰$ gives:

$$E_{OC} = 3 \times 10^3 \text{ m}^3 \cdot \text{s}^{-1}.$$

Using these values, the remaining coefficients can be derived from the long-term salt balance for each region (equations of the form of equation (13) for $S_{CCS}$, $S_{CCN}$, $S_{OCS}$, and $S_{OCN}$ with $dS/dt = 0$).

## SIMULATION OF SALINITY

The results of a simulation of the salt balance using the preceding model are shown in Fig. 13. The agreement between observed and computed data is generally good, not only for the mean values of salinity for each region, but also for the seasonal variations. To achieve this measure of agreement it was necessary to increase $E_{CCS}$ by 50% over the value computed using the long-term salt balance, and to increase $E_{IC}$ by 25%. Such trial and error adjustment is justified in view of the neglect of tidal pumping in the application of equation (10), and, more importantly, the neglect of correlations between $Q_f$ and $S$ in taking the long-term average of equation (13). The

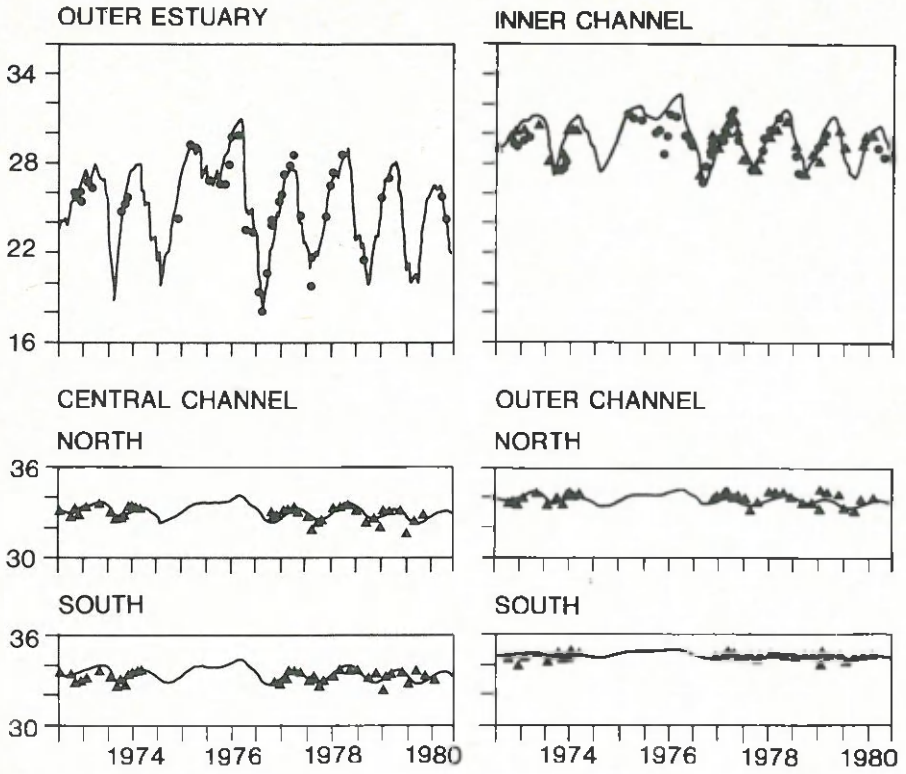


FIG. 13. Computed and observed salinities for the GEMBASE regions as functions of time. IMER data (▲), other sources (●).

agreement between observed and computed mean values of salinity for each region might be expected in view of the fact that these data were used in the process of defining mixing coefficients for the model. Nevertheless, the fact that seasonal variations are also reproduced with reasonable accuracy implies that the model has a substantial, although much simplified, physical basis.

Improvements between computed and observed data could possibly be achieved by incorporating wind-driven currents, or by further trial and error adjustment of the mixing coefficients.

## Discussion

This paper has demonstrated the value of a hydrodynamical model of the Bristol Channel for two problems in marine ecology. In the first of these, the model has been used to investigate the relationships between tidal stress and sediment bed-types, and between tidal stress and benthic macrofaunal associations. The model has also been used to infer the direction of sediment transport as bed-load (neglecting wind–wave effects), and to investigate the basic mechanism producing this transport, which is the result of asymmetry in the flood and ebb currents due to $M_4$ and residual currents.

The second problem concerns the definition of long-term transport for use in a coarse-lattice, ecosystem model of the Bristol Channel. The approach taken here is somewhat different from that taken by Kremer and Nixon (1978) in their ecosystem model of Narragansett Bay. In that work, fine-lattice hydrodynamical and water quality models were used together, in order to determine the transport (during the course of a day) between the eight large regions used to define their ecological model of the Bay. The daily exchanges between regions were tabulated as functions of tidal range on that day, and used to express the transport between regions during the course of an ecosystem simulation. The relevance of the tidal range can be seen from the flushing time of Narragansett Bay, which is about 30 d (two spring–neap cycles). The individual flushing times of each of the eight ecosystem regions will be much less than this. Therefore, the exchanges between regions will have a strong spring–neap tidal dependence. In contrast, the flushing time for the Severn Estuary is in the range 100–200 d (Uncles and Radford 1980), and the flushing times for the whole of the Channel will be much greater. Thus, variations over a spring–neap cycle will be rather small, and the dominant variations will be seasonal. For this reason, mixing coefficients and tidally induced residual flows for the Bristol Channel have been modeled as depending on average ($M_2$) tidal conditions. Freshwater-induced flows are highly seasonal in character, and are therefore treated as time-dependent. The method used by Kremer and Nixon (1978) suffers from difficulties at the open (seaward) boundaries of their fine-lattice hydrodynamical and water quality models. As with all such models of limited extent, conditions are not known exactly at the open boundaries, so that dispersive transport (mixing) across them is to some degree uncertain.

This has not been a difficulty with the Bristol Channel model, in which observed salinity data have been used to define the mixing.

The present ecological model does suffer from the limitation that mixing cannot be defined immediately in those situations where major alterations have occurred to the tidal currents, as would be the case with the introduction of, say, a tidal barrage. In these circumstances, residual currents can again be derived from the hydrodynamical model, but long-term, large-scale mixing coefficients would need to be defined from theoretical considerations. The most straightforward way of generating salinity data for the method would be through the application of a fine-lattice salinity model, the open boundaries of which extended some considerable distance into the Celtic Sea.

Although not reported here, the hydrodynamical model has also been used to investigate time-scales for vertical mixing in the Channel. These data have contributed to an understanding of phytoplankton dynamics in the highly turbid waters of the Severn Estuary and eastern Bristol Channel.

## Acknowledgments

I am grateful to Mr M. B. Jordan for his assistance with the field observations, and to Mr M. J. Howarth of the NERC Institute of Oceanographic Sciences, for permission to publish data from current meter station BID. Salinity data from GEMBASE simulations were kindly supplied by Mr P. J. Radford.

This work, which forms part of the estuarine ecology program of the Institute for Marine Environmental Research, a component of the Natural Environment Research Council (NERC), was partly supported by the Department of the Environment on Contract No DGR 480/48.

BELDERSON, R. H., AND A. H. STRIDE. 1966. Tidal current fashioning of a Basal Bed. Mar. Geol. 4: 237–257.

FISCHER, H. B., E. J. LIST, R. C. Y. KOH, J. IMBERGER, AND N. H. BROOKS. 1979. Mixing in inland and coastal waters. Academic Press, New York, NY. 484 p.

JOINT, I. R. 1983. The development of an ecosystem model of a turbid estuary. Can. J. Fish. Aquat. Sci. 40(Suppl. 1). (This issue)

KENYON, N. H. 1970. Sand ribbons of European tidal seas. Mar. Geol. 9: 25–39.

KREMER, J., AND S. W. NIXON. 1978. A coastal marine ecosystem. Ecol. Stud. 24: 250 p.

MILES, G. V. 1979. Estuarine modelling — Bristol Channel, p. 76–84. *In* R. T. Severn et al. [ed.] Tidal power and estuary management. Scientechnica.

PINGREE, R. D., AND D. K. GRIFFITHS. 1979. Sand transport paths around the British Isles resulting from $M_2$ and $M_4$ tidal interactions. J. Mar. Biol. Assoc. U.K. 59: 497–513.

PINGREE, R. D., AND L. MADDOCK. 1977. Tidal residuals in the English Channel. J. Mar. Biol. Assoc. U.K. 57: 339–354.

1978. The $M_4$ tide in the English Channel derived from a non-linear numerical model of the $M_2$ tide. Deep Sea Res. 25: 53–63.

PRANDLE, D. 1978. Residual flows and elevations in the southern North Sea. Proc. R. Soc. (A) 359: 189–228.

1980. Modelling of tidal barrier schemes: an analysis of the open-boundary problem by reference to AC circuit theory. Estuarine Coastal Mar. Sci. 11: 53–71.

RADFORD, P. J. 1979. Some aspects of an estuarine ecosystem model-GEMBASE, p. 301–322. *In* S. E. Jorgensen [ed.] State of the art in ecological modelling. Proceedings of the International Society for Ecological Modelling conference on ecological modelling, Copenhagen, 1978.

1981. Modelling the impact of a tidal power scheme on the Severn Estuary ecosystem. Paper presented at the International Symposium — Energy and Ecological Modelling, sponsored by the International Society for Ecological Modelling (Louisville, Kentucky, April 20–23, 1981). 13 p.

RADFORD, P. J., AND I. R. JOINT. 1980. The application of an ecosystem model to the Bristol Channel and Severn Estuary. Water Poliut. Control 79: 244–250.

RADFORD, P. J., R. J. UNCLES, AND A. W. MORRIS. 1981. Simulating the impact of technological change on dissolved cadmium distribution in the Severn Estuary. Water Res. 15: 1045–1052.

TEE, K. T. 1976. Tide-induced residual current, a 2-d non-linear numerical tidal model. J. Mar. Res. 34: 603–628.

UNCLES, R. J. 1981a. A numerical simulation of the vertical and horizontal $M_2$ tide in the Bristol Channel and comparisons with observed data. Limnol. Oceanogr. 26: 571–577.

1981b. A note on tidal asymmetry in the Severn Estuary. Estuarine Coastal Shelf Sci. 13: 419–432.

1982. Computed and observed residual currents in the Bristol Channel. Oceanol. Acta 5: 11–20.

UNCLES, R. J., AND M. B. JORDAN. 1979. Residual fluxes of water and salt at two stations in the Severn Estuary. Estuarine Coastal Mar. Sci. 9: 287–302.

UNCLES, R. J., AND P. J. RADFORD. 1980. Seasonal and spring–neap tidal dependence of axial dispersion coefficients in the Severn — a wide, vertically mixed estuary. J. Fluid Mech. 98: 703–726.

WARWICK, R. M., AND R. J. UNCLES. 1980. Distribution of benthic macrofauna associations in the Bristol Channel in relation to tidal stress. Mar. Ecol. Prog. Ser. 3: 97–103.